# MiR-155 promotes proliferation and inhibits apoptosis of nasopharyngeal carcinoma cells through targeting PTEN-PI3K/AKT pathway

W.-N. ZUO, H. ZHU, L.-P. LI, A.-Y. JIN, H.-Q. WANG

Department of Otorhinolaryngology, Cangzhou Central Hospital, Cangzhou, Hebei, China

**Abstract.** – OBJECTIVE: Nasopharyngeal carcinoma (NPC) is a polygenic hereditary disease, and the exact pathogenesis remains poorly understood. MiR-155 regulates the development and progression of several tumors. However, the role of MiR-155 in NPC has not been elucidated.

PATIENTS AND METHODS: The NPC cell line CNE2 was cultured *in vitro* and divided into control group, miR-155 mimics group, and miR-155 inhibitor group, followed by analysis of miR-155 expression by real-time PCR, cell proliferation by MTT assay, cell invasion by transwell chamber, Caspase3 activity, apoptosis of CNE2 cells by flow cytometry, and the expression of PTEN-PI3K/AKT signaling pathway by Western blot.

**RESULTS:** Transfection of miR-155 mimics significantly up-regulated miR-155 expression, promoted the proliferation and invasion of CNE2 cells, inhibited Caspase 3 activity, and decreased cell apoptosis, and PTEN expression, as well as increased PI3K/AKT phosphorylation compared with control group (p < 0.05). Transfection of miR-155 inhibitor inhibited the proliferation and invasion of CNE2 cells, increased Caspase 3 activity, cell apoptosis, and PTEN expression, as well as reduced PI3K/AKT phosphorylation. Compared with control group, the differences were statistically significant (p < 0.05).

CONCLUSIONS: Up-regulation of miR-155 can promote the proliferation of NPC cells and inhibit cell apoptosis by targeting the PTEN-PI3K/AKT pathway, thereby participating in the development and invasion of NPC, indicating that it might be a potential novel target for treating NPC.

Key Words:

MiR-155, PTEN, PI3K/AKT, Nasopharyngeal carcinoma, Proliferation, Apoptosis.

#### Introduction

Nasopharyngeal carcinoma (NPC) originates from the nasopharynx mucosal epithelial cells, and

its incidence is high, ranking first in otolaryngology malignant tumors1. Moreover, this incidence has regional and ethnic characteristics and family heredity, which occurs mostly in Southeast Asia. The nasopharyngeal carcinoma in China is more frequent in southern China, and the incidence rate in southern coastal cities is significantly higher than that in other regions<sup>2,3</sup>. At present, NPC is complicated by the composition of the nasopharynx, which is common in the top of the nasopharyngeal cavity, the pharyngeal crypt, and the sidewall. The site of the disease is deep and concealed, and the early progress is slow, which often leads to clinical misdiagnosis or delayed diagnosis, which increases the difficulty of treatment<sup>4,5</sup>. The treatment of nasopharyngeal carcinoma lacks individualized specific treatment methods and therapeutic drugs, mainly radiotherapy. Since most patients with NPC are already at an advanced stage, the treatment effect is not satisfactory with lower 5-year survival rate. The prognosis is poor especially in patients with advanced local metastasis of NPC<sup>5,6</sup>. In the occurrence and development of nasopharyngeal carcinoma, the pathogenic factors are complicated. Moreover, the NPC is affected by Epstein-Barr (EB) virus infection, genetic factors, dietary habits, and environmental factors, and belongs to polygenic hereditary diseases<sup>7,8</sup>. NPC involves a series of genetic changes, such as the activation of proto-oncogenes and/or the inactivation of tumor suppressor genes, which can disturb the physiological balance in the body, leading to abnormal cell proliferation, and thus promote the occurrence and development of tumors<sup>9,10</sup>. However, the exact pathogenesis of nasopharyngeal carcinoma has not been elucidated so far. Therefore, screening and identification of molecular markers specific for the early diagnosis of NPC have great significance to the early diagnosis and intervention.

Small molecule short-chain microRNAs (MiR-NAs) can be expressed in large numbers in cells

with a length of 18-25 nucleotides<sup>11</sup>. MiRNA binds to the 3' non-coding region of the corresponding target mRNA, thereby exerting an inhibitory effect on downstream transcriptional target genes<sup>12</sup>. MiRNA has up to 200 target genes and can be involved in the regulation of several diseases<sup>13</sup>. MicroRNAs play a role in tumorigenesis and can act as tumor markers, as oncogenes that promote tumor growth or as tumor suppressor genes that inhibit the growth of latent malignant cells<sup>14</sup>. MiR-155 is expressed in multiple organs such as the thymus and spleen, and has been shown to be highly expressed in various tumors such as lung cancer and breast cancer<sup>15,16</sup>. However, the expression and mechanism of miR-155 in nasopharyngeal carcinoma cells have not been fully elucidated. Therefore, the aim of this investigation is to explore the role of miR-155 in the development and progression of nasopharyngeal carcinoma.

## **Materials and Methods**

#### Main Reagents and Instruments

The nasopharyngeal carcinoma cell line CNE2 was preserved in our laboratory and stored in liquid nitrogen. Dulbecco's Modified Eagle's Medium (DMEM), fetal bovine serum (FBS), and cyan chain double antibody were purchased from HyClone (South-Logan, UT, USA). Dimethyl sulfoxide (DMSO), MTT (3-(4,5-dimethylthiazol-2-vl)-2,5-diphenyl tetrazolium bromide) powder was purchased from Gibco (Grand Island, NY, USA); ethylenediaminetetraacetic acid (EDTA) digest was purchased from Sigma-Aldrich (St. Louis, MO, USA). Polyvinylidene difluoride (PVDF) membrane was purchased from Pall Life Sciences (Port Washington, NY, USA), EDTA was purchased from HyClone (South-Logan, UT, USA), and Western blot related chemical reagent was purchased from Shanghai Biyuntian Biotechnology Co., Ltd. (Shanghai, China); enhanced chemiluminescence (ECL) reagent was purchased from Amersham Biosciences (Little Chalfont, Buckinghamshire, UK), rabbit anti-human phosphatase and tensin homolog (PTEN) monoclonal antibody, rabbit anti-human p -AKT, p-PI3K, MMP2, AKT, PI3K mAb, and mouse anti-rabbit horseradish peroxidase (HRP)-labeled IgG secondary antibody were purchased from Cell Signaling Technology (Danvers, MA, USA). The transwell chamber was purchased from Corning (Corning, NY, USA). The Caspase3 active kit was purchased from Nanjing Jiancheng

Company (Nanjing, China). The RNA extraction kit, reverse transcription kit, and lipo2000 reagent were purchased from Invitrogen (Carlsbad, CA, USA). TagMan MicroRNA Reverse Transcription Kit was purchased from Thermo Fisher Scientific (Waltham, MA, USA). MiR-155 mimics and inhibitors were synthesized by Shanghai Jima Pharmaceutical Technology Co., Ltd (Shanghai, China). Other commonly used reagents were purchased from Shanghai Shenggong Biological Co., Ltd (Shanghai, China). The ultra-clean workbench was purchased from Suzhou Sutai Purification Equipment Engineering Co., Ltd (Suzhou, China). Thermo Scientific Forma Carbon Dioxide (CO<sub>2</sub>) incubator was purchased from Thermo Fisher Scientific (Waltham, MA, USA). ABI 7700 Fast Quantitative PCR Reactor was purchased from ABI (Waltham, MA, USA). The inverted microscope was purchased from Olympus Corporation (Shinjuku, Tokyo, Japan).

## CNE2 Cell Culture and Grouping

The liquid nasopharyngeal carcinoma cell line CNE2 was stored in liquid nitrogen, thawed in a 37°C water bath. When the cells were completely thawed, they were centrifuged at 1000 rpm for 3 min and resuspended in 1 ml of fresh DMEM medium, transferred to a 5 ml cell culture flask containing 2 ml of fresh DMEM medium, and cultured at 37°C with 5% CO, in a saturated humidity incubator for 24-48 h. The CNE2 cells were seeded in a culture dish at 1×10<sup>6</sup> cells/cm<sup>2</sup> containing 10% fetal bovine serum (FBS), 90% high glucose DMEM medium (containing 100 U/ml penicillin, 100 µg/ ml streptomycin), and cultured at 37°C with 5% CO<sub>2</sub>. The study used 3-8 generation logarithmic growth phase cells. Cultured CNE2 cells were randomly divided into 3 groups, control group, miR-155 mimics group, and miR-155 inhibitor group.

# Liposome Transfection of MiR-155 Mimics and MiR-155 Inhibitor

MiR-155 mimics and miR-155 inhibitor were transfected into CNE2 cells, respectively. The miR-155 mimics sequence was 5'-GAUCGGU-AGUUGUGCACA-3'. The miR-155 inhibitor sequence was 5'-CGGAGUGCAUAUGUGCUA-3'. The cell density was fused to 70-80%; the miR-155 mimics and miR-155 inhibitor, and the negative control liposome were separately added to 200 μl of serum-free DMEM medium, mixed well, and incubated at room temperature for 15 min. The mixed lipo2000 was mixed with miR-155 mimics and miR-155 inhibitor dilutions, and incubated

for 30 min at room temperature. The serum of the cells was removed, and cells were rinsed with PBS followed by addition of 1.6 ml serum-free DMEM medium and cultured in a 5% CO<sub>2</sub> incubator. The serum culture solution was changed at 37°C for 6 h, and the culture was further continued for 48 h.

# Real-Time PCR Detection of MiR-155 Expression

Total RNA was extracted using TRIzol reagent, and DNA reverse transcription synthesis was performed according to the kit instructions. The primers were designed by Primer Premier 6.0 according to each gene sequence and synthesized by Shanghai Yingjun Biotechnology Co., Ltd. (Table I). Real-time PCR was conducted for detection of the gene of interest with reaction conditions as follows: 55°C 1 min, 92°C 30 s, 58°C 45 s, 72°C 35 s, a total of 35 cycles. Glyceraldehyde 3-phosphate dehydrogenase (GAPDH) was used as a reference. According to the fluorescence quantification, the starting cycle number (CT) of all samples and standards was calculated. Based on the standard CT value, a standard curve was drawn, and then the semi-quantitative analysis was carried out using the 2- $\Delta$ Ct method.

#### MTT Assay to Detect Cell Proliferation

The logarithmic growth phase CNE2 cells were collected from DMEM medium containing 10% fetal bovine serum in a 96-well culture plate at a cell number of  $5\times10^3$ , and the supernatant was discarded after 24 h of culture. Cells in each group were treated at intervals of 24 h followed by the addition of 20  $\mu$ l of sterile MTT. 3 replicate wells were set at each time point. After 4 h of continuous culture, the supernatant was completely removed, and dimethyl sulfoxide (DMSO) 150  $\mu$ l/well was added for 10 min incubation. When the purple crystals were fully dissolved, the absorbance (A) value was measured at a wavelength of 570 nm to reflect cell proliferation.

# Transwell Chamber to Detect Cell Invasion

After 48 h of transfection, cells in each group were cultured in Dulbecco's Modified Eagle's

Medium (DMEM) containing 10% fetal bovine serum (FBS), and, then, cultured for 24 h in serum-free DMEM medium. The bottom of the transwell chamber and the upper chamber of the membrane were coated with 50 mg/L Matrigel 1:5 dilution and air-dried at 4°C. The residual liquid in the plate was aspirated, and 50 µl of serum-free medium containing 10 g/L of bovine serum albumin (BSA) was added to each well and incubated at 37°C for 30 min. The transwell chamber was placed in a 24-well culture plate, and 500 µl of DMEM medium containing 10% fetal bovine serum was added to the small chamber, followed by addition of 100 µl tumor cell suspension to the chamber and cultured in serum-free DMEM medium. At the same time, cells in the same conditions were added to the transwell chamber without Matrigel as a control. The cells were cultured for 48 h. The transwell chamber was taken out, rinsed with PBS, and cells in the upper layer of the microporous membrane were wiped off with a cotton swab, fixed in ice ethanol, and stained with crystal violet for 30 min. The cells transferred to the lower layer of the microporous membrane were counted under an inverted microscope. 10 fields of view were counted for each sample, and the average was calculated.

#### Western Blot

The total protein of each group was extracted: the lysate was added, the cells were lysed on ice for 15-30 min, the cells were disrupted by sonication for 5 s  $\times$  4 times, centrifuged at  $4^{\circ}$ C, 10 000 × g for 15 min, and the supernatant was transferred to a new Eppendorf (EP) tube followed by quantification of the protein concentration by the bicinchoninic acid (BCA) assay which was stored at -20°C for Western blot experiments. The isolated protein was electrophoresed on a 10% sodium dodecyl sulphate-polyacrylamide gel electrophoresis (SDS-PAGE), transferred to a PVDF membrane by semi-dry transfer, blocked with 5% skim milk powder for 2 h and incubated with primary antibody 1:2000, 1:2000, 1:1000, 1:1500, 1:1000 diluted p-AKT, p-PI3K, PTEN, AKT,

Table I. Primers sequences.

Gene	Forward 5'-3'	Reverse 5'-3'
GAPDH	AGTACCGTCTAGTCTGG	TAATAGAATGTCGGCTGGT
Mir-155	CCTACAGACCCTCTGTAAG	GCATTCCGACTGGGTATGATT

PI3K monoclonal antibody at 4°C overnight. After Phosphate-Buffered Saline and Tween 20 (PBST) washing, the membrane was incubated with 1:2000 diluted goat anti-rabbit secondary antibody for 30 min followed by washing with PBST and addition of chemiluminescence for 1 min. Then, the membrane was exposed and developed. X-film and strip density measurements were separately scanned using protein image processing system software and Quantity one software. The experiment was repeated four times (n=4).

## Caspase3 Activity Detection

The changes in Caspase3 activity in each group of cells were assessed according to the kit instructions. Trypsin-digested cells were centrifuged at 600 g at 4°C for 5 min, followed by the addition of cell lysate and lysed on ice for 15 min. After that, cells were centrifuged at 20000 g at 5°C for 5 min and 2 mM Ac-DEVD-pNA was added to measure optical density (OD) at 405 nm wavelengths to reflect Caspase3 activity.

## Flow Cytometry Analysis of Cell Apoptosis

Tumor cells were digested, counted, and inoculated into 50 mL culture flasks at a concentration of 5×10<sup>5</sup>/mL, and randomly divided into 3 groups with treatment being mentioned above, with 3 bottles in each group. After transfection treatment for 48 h, the cells were counted after routine digestion, and the cells of each group

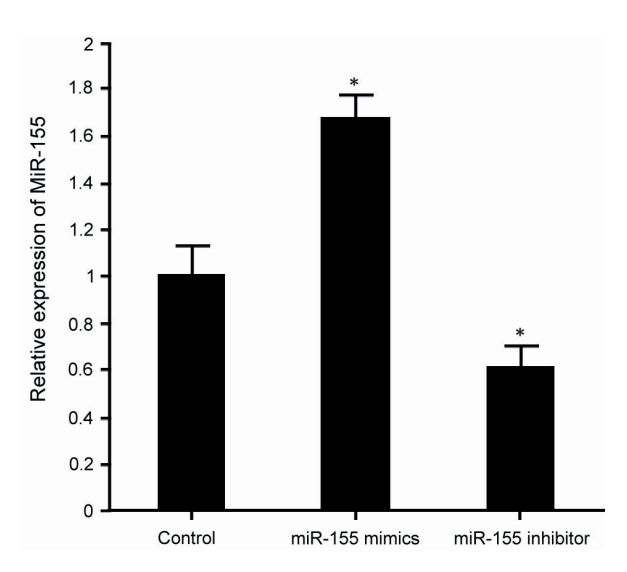


**Figure 1.** Effect of miR-155 on the expression of miR-155 in nasopharyngeal carcinoma cell line CNE2. Compared with the control group, \*p < 0.05.

were collected. The number of cells collected was about  $2\times10^6$ , and washed with  $1\times PBS$ , fixed with pre-cooled 75% ethanol, and incubated overnight at 4°C. After  $1\times PBS$  washing, cells were resuspended in a mixed solution of 800  $\mu$ l  $1\times PBS$  and 1% bovine serum albumin (BSA) followed by addition of  $100~\mu g/ml$  propidium iodide (PI) solution (3.8% Sodium Citrate, pH 7.0) and 100~RNAase (RnaseA, 10~mg/ml) and incubated at  $37^{\circ}C$  for 30~min under the dark. Then, cell apoptosis was detected by flow cytometry.

#### Statistical Analysis

All data are expressed as mean  $\pm$  standard deviation (SD). The mean values of the two groups were compared by Student's *t*-test test and analyzed by SPSS 11.5 software (SPSS Inc., Chicago, IL, USA). The differences between groups were analyzed by analysis of variance (ANOVA) and Dunnett's test. p < 0.05 was a statistically significant difference.

#### Results

# Effect of MiR-155 on MiR-155 Expression in CNE2 Cells

The effect of transfection of miR-155 mimic and inhibitor on the expression of mir-155 in nasopharyngeal carcinoma cell CNE2 was detected by Real-Time PCR. The results showed that transfection of miR-155 mimics in CNE2 cells significantly promoted the expression of miR-155 compared with control group (p < 0.05). Transfection of miR-155 inhibitor in CNE2 cells significantly inhibited the miR-155 expression (p < 0.05; Figure 1).

# Effect of MiR-155 on the Proliferation of CNE2 Cells

The effects of transfection of miR-155 mimic and inhibitor on the proliferation of CNE2 cells were detected by MTT assay. Transfection with miR-155 mimic significantly promoted the proliferation of CNE2 cells compared with control group (p < 0.05). Whereas, miR-155 inhibitor transfection significantly inhibited the proliferation of CNE2 cells (p < 0.05; Figure 2).

# Effect of MiR-155 on Caspase3 Activity in CNE2 Cells

When transfected with miR-155 mimic to promote the expression of miR-155, Caspase 3 activity was significantly inhibited (p < 0.05). When transfected with miR-155 inhibitor to inhibit the

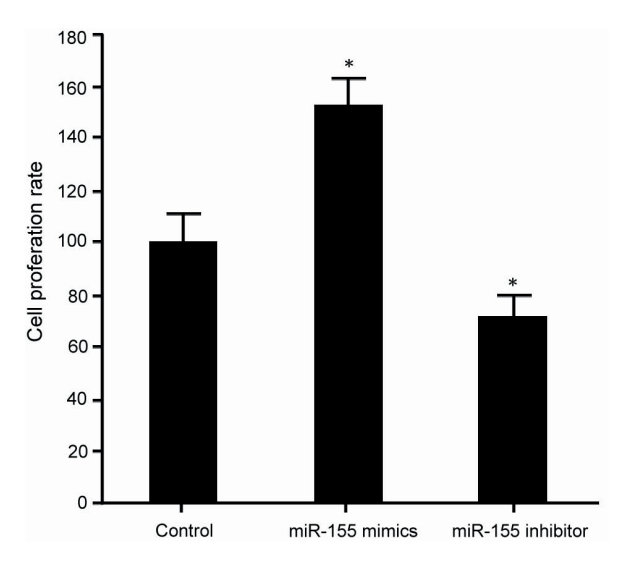


**Figure 2.** Effect of miR-155 on the proliferation of nasopharyngeal carcinoma CNE2 cells. Compared with the control group, \* p < 0.05.

expression of miR-155, Caspase 3 activity was significantly increased (p < 0.05) (Figure 3).

# Effect of MiR-155 on Apoptosis of CNE2 Cells

In CNE2 cells transfected with miR-155 mimic, the apoptosis rate of tumor cells was significantly inhibited compared with control group (p < 0.05). However, in CNE2 cells transfected with miR-155 inhibitor, the apoptosis of tumor cells was significantly increased (p < 0.05; Figure 4).

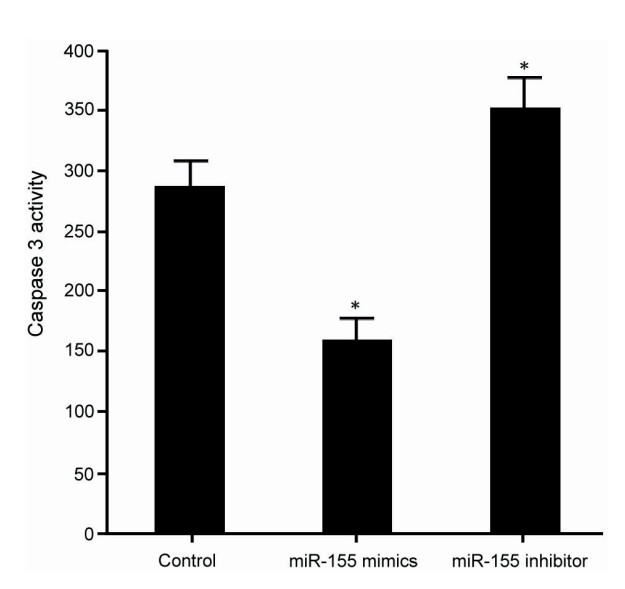


**Figure 3.** Effect of miR-155 on caspase3 activity in nasopharyngeal carcinoma CNE2 cells. Compared with the control group, \* p < 0.05.

# Effect of MiR-155 on Invasion of CNE2 Cells

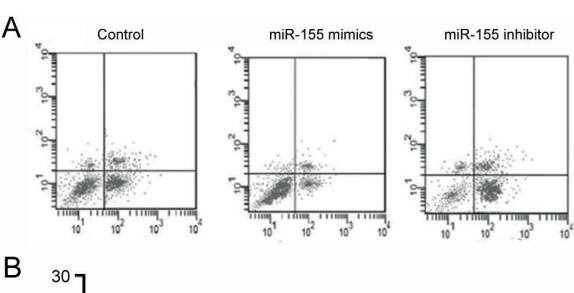
Transwell chamber analysis showed that, when miR-155 mimic was transfected to promote the expression of miR-155 in CNE2 cells, it could significantly promote tumor cell invasion (p < 0.05). When miR-155 expression in carcinoma CNE2 cells was inhibited, the invasion of tumor cells was significantly decreased (p < 0.05; Figure 5).

# Effect of MiR-155 on the Expression of PTEN-PI3K/AKT in CNE2 Cells

Transfection of miR-155 mimics decreased PTEN expression and increased PI3K/AKT phosphorylation. Whereas, transfection of miR-155 inhibitor increased the expression of PTEN and decreased the expression of PI3K/AKT phosphorylation (Figure 6).

# Discussion

Nasopharyngeal carcinoma is concealed due to its location. Most patients are already in advanced



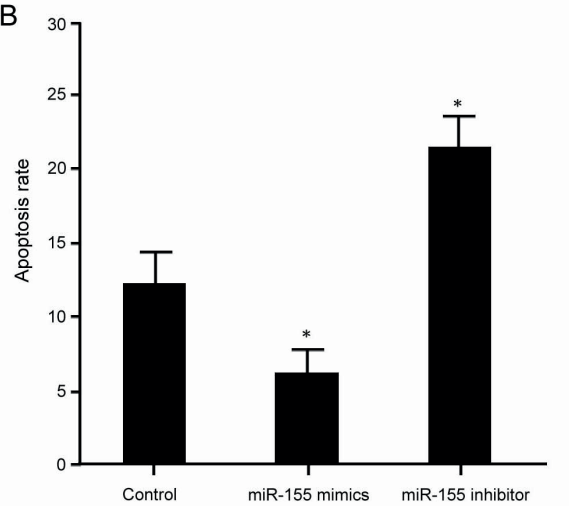


**Figure 4.** Effect of miR-155 on apoptosis of nasopharyngeal carcinoma CNE2 cells. **A,** Flow cytometry regulates the effect of miR-155 on apoptosis of nasopharyngeal carcinoma CNE2 cells; **B,** Cell apoptosis rate analysis; comparison of control group, \* p < 0.05.

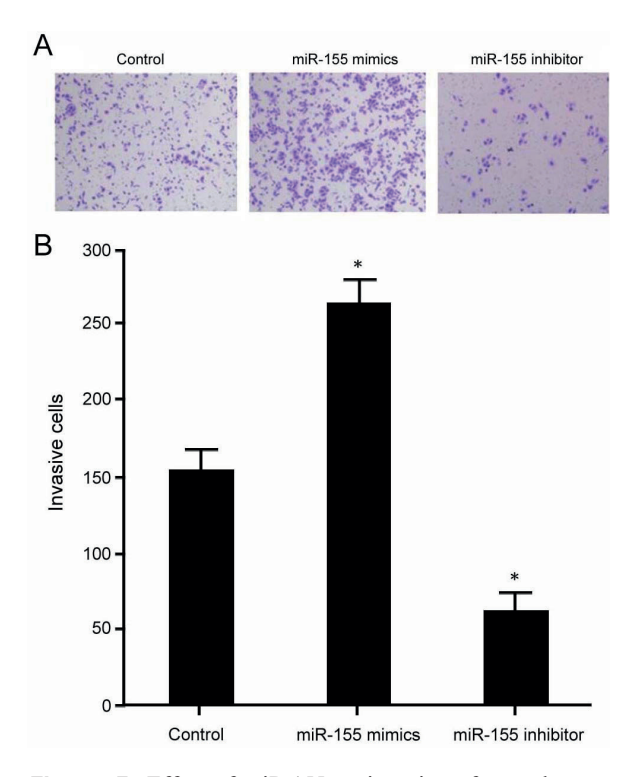


**Figure 5.** Effect of miR-155 on invasion of nasopharyngeal carcinoma CNE2 cells. **A**, Transwell chamber analysis regulates the effect of miR-155 on invasion of nasopharyngeal carcinoma CNE2 cells (x100); **B**, Cell invasion ability analysis; comparison of control group, \* p < 0.05.

stage at the time of receiving treatment, and most NPC is a poorly differentiated non-keratinized squamous cell carcinoma with high malignancy, strong invasive ability, and easy metastasis<sup>17</sup>. Therefore, NPC often requires radiotherapy for treatment, but is not sensitive to other treatment methods. Determining effective molecular markers can help evaluate the treatment efficacy and prognosis of patients with nasopharyngeal carcinoma, and help individualized treatment, which might bring new hope for the diagnosis and treatment of clinical nasopharyngeal carcinoma<sup>18</sup>.

Small molecule nucleotide MiRNA has a wide range of regulatory functions and plays an important role in physiological and pathological environments, and can be involved in biological processes such as cell proliferation, differentiation, and apoptosis<sup>19</sup>. The transcriptional regulation level, pathological state, environmental changes, and other factors can lead to changes of MiRNA expression, so the expression and regulation mechanisms of MiRNA may be different<sup>20</sup>. MiRNA is associated with a variety of diseases, and it is closely related to tumors. It is an important tar-

get in the diagnosis and prognosis of tumors and has become a research hotspot in recent years<sup>21</sup>. The results of this study showed that increase of miR-155 expression in nasopharyngeal carcinoma cells can promote tumor cell proliferation and invasion, decrease caspase activity, increase apoptosis rate, whereas, inhibition of the expression of miR-155 in NPC cells inhibits tumor cell proliferation and invasion, increases Caspase activity, and reduces cell apoptosis, which is similar to the expression and effect of miR-155 in other tumors<sup>15</sup>. The most active Caspase apoptosis family is Caspase 3, which is an executive factor of cell apoptosis. Increased Capspase3 activity can induce tumor cell apoptosis<sup>22</sup>. The results suggest that the development and progression of NPC can play a role in promoting cancer, which can promote the proliferation of NPC cells, inhibit cell apoptosis, and promote invasion and metastasis.

PTEN is a tumor suppressor gene and belongs to a class of genes that negatively regulate cell

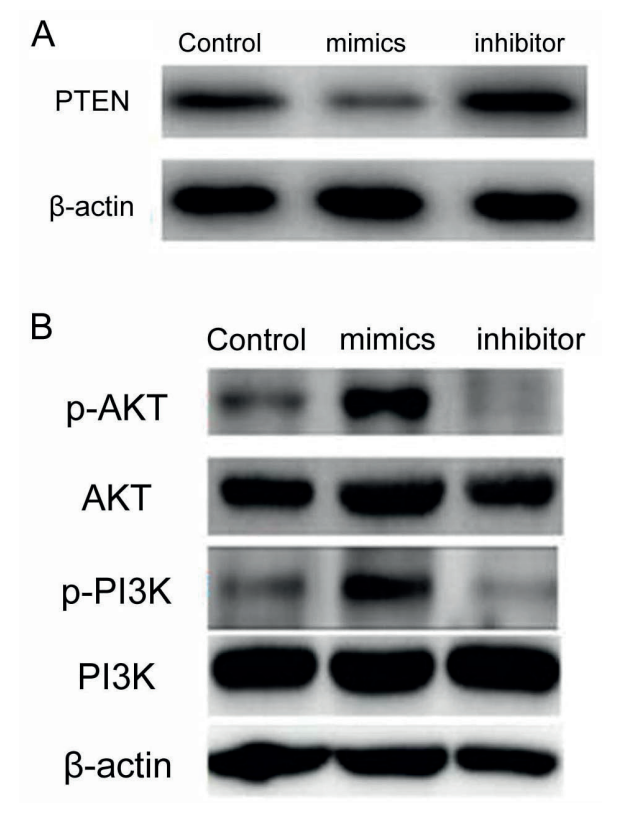


**Figure 6.** Effect of miR-155 on the expression of PTEN-PI3K/AKT in nasopharyngeal carcinoma CNE2 cells. **A**, Effect of regulation of miR-155 on PTEN expression in nasopharyngeal carcinoma CNE2 cells; **B**, Effect of regulation of miR-155 on PI3K/AKT expression in nasopharyngeal carcinoma CNE2 cells.

proliferation. It can inhibit the development of tumors by antagonizing the activity of phosphorylases such as tyrosine kinases<sup>23</sup>. The AKT/ PI3K signaling pathway is closely related to tumorigenesis, and its activation can lead to tumor cell proliferation, cell cycle, and progression. Studies<sup>24,25</sup> have confirmed that nasopharyngeal carcinoma progression is associated with AKT/ PI3K signaling pathway. This study further investigated its mechanism and found that up-regulation of miR-155 expression in nasopharyngeal carcinoma CNE2 cells leads to decreased PTEN expression and increased PI3K/AKT phosphorylation. Inhibition of miR-155 expression in CNE2 cells promoted the increase of PTEN expression and decreased phosphorylation of PI3K/ AKT. This result indicates that miR-155 is closely related to PTEN-PI3K/AKT regulation. At present, the mechanism of miR-155 in regulating the proliferation and apoptosis of NPC cells is rare. This study intends to further analyze the expression profile of miR-155 in tumor tissues of patients with clinical NPC and its correlation with treatment prognosis, and analyze its possible mechanism, which provides a new theoretical basis for clinical diagnosis and treatment of nasopharyngeal carcinoma.

## Conclusions

The up-regulation of miR-155 promoted the proliferation of nasopharyngeal carcinoma cells and inhibited the apoptosis of NPC cells, which is possible by targeting the PTEN-PI3K/AKT pathway, thus participating in the process of invasion and metastasis of NPC. The proliferation of cancer cells promoted apoptosis and inhibited the occurrence and invasion of nasopharyngeal carcinoma. Therefore, miR-155 might be used as a new molecular target for the diagnosis and treatment of nasopharyngeal carcinoma.

## **Conflict of Interests**

The Authors declare that they have no conflict of interests.

## References

 PENG H, DONG D, FANG MJ, LI L, TANG LL, CHEN L, LI WF, MAO YP, FAN W, LIU LZ, TIAN L, LIN AH, SUN Y, TIAN J, MA J. Prognostic value of deep learning pet/ ct-based radiomics: potential role for future individual induction chemotherapy in advanced naso-

- pharyngeal carcinoma. Clin Cancer Res 2019; 25: 4721-4279.
- ZHOU J, ZHANG J, XU M, KE Z, ZHANG W, MAI J. High SRC-1 and Twist1 expression predicts poor prognosis and promotes migration and invasion by inducing epithelial-mesenchymal transition in human nasopharyngeal carcinoma. PLoS One 2019; 14: e0215299.
- Wang LQ, Deng AC, Zhao L, Li Q, Wang M, Zhang Y. Mir-1178-3p promotes the proliferation, migration and invasion of nasopharyngeal carcinoma sune-1 cells by targeting STK4. J Biol Regul Homeost Agents 2019; 33: 321-330.
- 4) ZHAO C, MIAO JJ, HUA YJ, WANG L, HAN F, LU LX, XIAO WW, WU HJ, ZHU MY, HUANG SM, LIN CG, DENG XW, XIE CH. Locoregional control and mild late toxicity after reducing target volumes and radiation doses in patients with locoregionally advanced nasopharyngeal carcinoma treated with induction chemotherapy (IC) followed by concurrent chemoradiotherapy: 10-year results of a phase 2 study. Int J Radiat Oncol Biol Phys 2019; 104: 836-844.
- Yugui F, Wang H, Sun D, Zhang X. Nasopharyngeal cancer combination chemoradiation therapy based on folic acid modified, gefitinib and yttrium 90 co-loaded, core-shell structured lipid-polymer hybrid nanoparticles. Biomed Pharmacother 2019; 114: 108820.
- 6) ZHOU Z, MENG M, NI H. Chemosensitizing effect of astragalus polysaccharides on nasopharyngeal carcinoma cells by inducing apoptosis and modulating expression of bax/bcl-2 ratio and caspases. Med Sci Monit 2017; 23: 462-469.
- CHEN Z, GUO Q, Lu T, LIN S, ZONG J, ZHAN S, Xu L, PAN J. Pretreatment serum lactate dehydrogenase level as an independent prognostic factor of nasopharyngeal carcinoma in the intensity-modulated radiation therapy era. Med Sci Monit 2017; 23: 437-445.
- 8) Meng DF, Xie P, Peng LX, Sun R, Luo DH, Chen QY, Lv X, Wang L, Chen MY, Mai HQ, Guo L, Guo X, Zheng LS, Cao L, Yang JP, Wang MY, Mei Y, Qiang YY, Zhang ZM, Yun JP, Huang BJ, Qian CN. CDC42-interacting protein 4 promotes metastasis of nasopharyngeal carcinoma by mediating invadopodia formation and activating EGFR signaling. J Exp Clin Cancer Res 2017; 36: 21.
- 9) MAO L, TAN J, WANG F, LUO Y, LIU W, ZENG F, YU B, HUANG H, LU J, PENG X, LIU X. Retrospective study comparing anti-EGFR monoclonal antibody plus cisplatin-based chemoradiotherapy versus chemoradiotherapy alone for stage ii-ivb nasopharyngeal carcinoma and prognostic value of EGFR and VEGF expression. Clin Otolaryngol 2019; 44: 572-580.
- Liu J, Liu Y, Zhang Z, Sun H, Ji X, Li B, Zhou X, Gai P. Prognostic value of the epstein-barr virus and tumor suppressor gene p53 gene in nasopharyngeal squamous cell carcinoma. J Cancer Res Ther 2019; 15: 426-436.
- 11) ZHANG Y, ZENG Z, CHEN C, LI C, XIA R, LI J. Genome-wide characterization of the auxin response

- factor (ARF) gene family of litchi (litchi chinensis sonn.): Phylogenetic analysis, miRNA regulation and expression changes during fruit abscission. PeerJ 2019; 7: e6677.
- 12) HE C, CHEN ZY, LI Y, YANG ZQ, ZENG F, CUI Y, HE Y, CHEN JB, CHEN HQ. Mir-10b suppresses cell invasion and metastasis through targeting HOXA3 regulated by FAK/YAP signaling pathway in clear-cell renal cell carcinoma. BMC Nephrol 2019; 20: 127.
- OH YS, BAE GD, PARK EY, Jun HS. MicroRNA-181c inhibits interleukin-6-mediated beta cell apoptosis by targeting TNF-alpha expression. Molecules 2019; 24. pii: E1410.
- 14) Zhao X, Feng J, Zhang L, Zhao F, Li M, Du Y, Li Y, Wu Q, Li G. One functional variant in the 3'-untranslated region of TLR is associated with the elevated risk of ventilator-associated pneumonia in the patients with chronic obstructive pulmonary disease. J Cell Physiol 2019; 234: 18879-18886.
- 15) FERNANDEZ C, BELLOSILLO B, FERRARO M, SEOANE A, SANCHEZ-GONZALEZ B, PAIRET S, PONS A, BARRANCO L, VELA MC, GIMENO E, COLOMO L, BESSES C, NAVARRO A, SALAR A. MicroRNAs 142-3p, mir-155 and mir-203 are deregulated in gastric MALT lymphomas compared to chronic gastritis. Cancer Genomics Proteomics 2017; 14: 75-82.
- 16) CAO S, WANG Y, LI J, LV M, NIU H, TIAN Y. Tumor-suppressive function of long noncoding RNA MALAT1 in glioma cells by suppressing mir-155 expression and activating FBXW7 function. Am J Cancer Res 2016; 6: 2561-2574.
- 17) Wang YH, Yin YW, Zhou H, Cao YD. Mir-639 is associated with advanced cancer stages and promotes proliferation and migration of nasopharyngeal carcinoma. Oncol Lett 2018; 16: 6903-6909.
- 18) Yiu SPT, Hui KF, Choi CK, Kao RYT, Ma CW, Yang D, Chiang AKS. Intracellular iron chelation by a novel compound, C7, reactivates epstein barr virus (EBV) lytic cycle via the ERK-autophagy axis in

- EBV-positive epithelial cancers. Cancers (Basel) 2018; 10. pii: E505.
- 19) TARVER JE, CORMIER A, PINZON N, TAYLOR RS, CARRE W, STRITTMATTER M, SEITZ H, COELHO SM, COCK JM. MicroRNAs and the evolution of complex multicellularity: identification of a large, diverse complement of microRNAs in the brown alga ectocarpus. Nucleic Acids Res 2015; 43: 6384-6398.
- NADIM WD, SIMION V, BENEDETTI H, PICHON C, BARIL P, MORISSET-LOPEZ S. MicroRNAs in neurocognitive dysfunctions: new molecular targets for pharmacological treatments? Curr Neuropharmacol 2017; 15: 260-275.
- 21) Bosia C, Sgrò F, Conti L, Baldassi C, Brusa D, Cavallo F, Cunto FD, Turco E, Pagnani A, Zecchina R. RNAs competing for micrornas mutually influence their fluctuations in a highly non-linear microRNA-dependent manner in single cells. Genome Biol 2017; 18: 37.
- 22) LEE HS, CHEERATHODI M, CHAKI SP, REYES SB, ZHENG Y, Lu Z, PAIDASSI H, DERMARDIROSSIAN C, LACY-HULBERT A, RIVERA GM, McCARTY JH. Protein tyrosine phosphatase-PEST and β8 integrin regulate spatiotemporal patterns of RhoGDI1 activation in migrating cells. Mol Cell Biol 2015; 35: 1401-1413.
- 23) JAVADI A, DEEVI RK, EVERGREN E, BLONDEL-TEPAZ E, BAIL-LIE GS, SCOTT MG, CAMPBELL FC. PTEN controls glandular morphogenesis through a juxtamembrane beta-arrestin1/ARHGAP21 scaffolding complex. Elife 2017; 6. pii: e24578.
- 24) Dong P, Hao F, Dai S, Tian L. Combination therapy Eve and Pac to induce apoptosis in cervical cancer cells by targeting PI3K/AKT/mTOR pathways. J Recept Signal Transduct Res 2018; 38: 83-88.
- 25) SOLIMAN M, SEO JY, KIM DS, KIM JY, PARK JG, ALFAJARO MM, BAEK YB, CHO EH, KWON J, CHOI JS, KANG MI, PARK SI, CHO KO. Activation of PI3K, AKT, and ERK during early rotavirus infection leads to V-ATPase-dependent endosomal acidification required for uncoating. PLoS Pathog 2018; 14: e1006820.